Hindawi Publishing Corporation
International Journal of Photoenergy
Volume 2015, Article ID 147836, 8 pages
http://dx.doi.org/10.1155/2015/147836

Research Article

Optical Properties of Spin-Coated TiO_2 Antireflection Films on Textured Single-Crystalline Silicon Substrates

Ryosuke Watanabe, Yohei Eguchi, Takuya Yamada, and Yoji Saito

Department of Systems Design Engineering, Seikei University, 3-3-1 Kichijoji-kitamachi, Musashino, Tokyo 180-8633, Japan

Correspondence should be addressed to Ryosuke Watanabe; rwatanabe@st.seikei.ac.jp

Received 15 June 2014; Revised 3 September 2014; Accepted 6 September 2014

Academic Editor: Vincenzo Augugliaro

Antireflection coating (ARC) prepared by a wet process is beneficial for low cost fabrication of photovoltaic cells. In this study, we investigated optical properties and morphologies of spin-coated TiO_2 ARCs on alkaline textured single-crystalline silicon wafers. Reflectance spectra of the spin-coated ARCs on alkaline textured silicon wafers exhibit no interferences and low reflectance values in the entire visible range. We modeled the structures of the spin-coated films for ray tracing numerical calculation and compared numerically calculated reflectance spectra with the experimental results. This is the first report to clarify the novel optical properties experimentally and theoretically. Optical properties of the spin-coated ARCs without interference are due to the fractional nonuniformity of the thickness of the spin-coated ARCs that cancels out the interference of the incident light.

1. Introduction

Light reflection reduction from a surface of photovoltaic cells is a key technology to increase light harvesting performance of the cells and to improve cell efficiency. For single-crystalline Si photovoltaic cells with an (100) orientation, alkaline etching of the substrates to form pyramidal-surface-textured structures is widely accepted. In addition, to reduce surface reflection, antireflection coatings (ARCs) are typically formed on the textured area.

Chemical vapor deposition (CVD) is commonly used to form ARCs on the textured or flat silicon wafers [1–5]. Dielectric layers such as SiO_2 [2], SiN [4], and TiO_2 [2, 5] with several tens of nanometers are deposited uniformly onto the wafers. The ARCs deposited by CVD methods perform satisfactorily and have been commercially adopted; however, the CVDs are expensive, because they need an expensive high vacuum system.

Wet processes such as sol-gel spin-coating and dip coating methods cost-effectively form ARCs on the wafers [6, 7], because these methods do not need expensive equipment and running cost which are lower than those of CVD methods. Attention has recently been paid to sol-gel methods for forming ARCs on the flat-surface solar cells [8, 9]. However, there have been few studies about forming ARCs on the textured silicon wafers using sol-gel methods. San Vicente et al. first reported the sol-gel ARC for textured monocrystalline silicon substrates [10]. Arabi et al. prepared the sol-gel ARC for polycrystalline silicon [11]. Petersson et al. compared the optical properties of ARCs, which consist of TiO_2 and SiO_2 [12]. Yang et al. investigated ARCs, which consist of a SiO_2-TiO_2 mixture for multicrystalline textured silicon cells [13]. However, details of the optical properties and structures of sol-gel deposited ARC films have not yet been thoroughly investigated. In this study, we observed the morphology of the spin-coated antireflection films on textured substrates. We measured and calculated the reflectance to investigate the detailed optical properties of the sol-gel deposited films.

2. Experimental Procedure

In this study, we used n-type single-crystalline Si substrates (100) with the thickness of 625 ± 25 μm and resistivity of 1 to 10 Ωcm. At first, the substrates were cut to 30 mm × 22 mm, dipped into a diluted BHF solution, and then rinsed

with deionized water (DIW). Next, the wafers were etched with alkaline solution ($KOH : H_2O = 1:1$) for 10 min and rinsed with DIW. Then the wafers were textured with another alkaline solution ($KOH : C_3H_8O : H_2O = 1:2:44$) for 30 min at 70°C, where the solution was stirred using a magnetic stirrer [14]. After texturing, the wafers were rinsed again with DIW. Periodic size of the formed textured structures was around 2 to 5 μm in our conditions.

Commercially available TiO_2 sol-gel solution (Ti-03-P, Kojundo Chemical Laboratory Co., Ltd.) was used in the experiment. Solutions were dropped onto the textured substrates and spin-coated at 3000 rpm. After spin-coating, the wafers were dried on a hot plate at 120°C for 5 min, followed by heat-burning at 500°C for 20 min in air.

Refractive indices of the coated TiO_2 films were examined by a spectroscopic ellipsometer (M-2000, J. A. Woollam Co.). The ellipsometry measurements were performed for the TiO_2 films on flat silicon wafers. Morphology of the textured surfaces was observed with scanning electron microscopy (SEM, TB-6360 and JSM-7001F, JEOL Ltd.). Also, elemental analysis was carried out with SEM-EDS (JSM-7001F, JEOL Ltd.). Optical reflections were measured using a double beam spectrometer (U-3000, Hitachi High-Technologies Co.) with an integrating sphere. For reflection measurements, an angle spacer was used for preventing specular reflection.

3. Numerical Calculations

We used a two-dimensional finite difference time domain (FDTD) method for evaluating light reflection from the sample surface. The FDTD method directly calculates Maxwell's equations, and there are no approximations in principle. Therefore, the FDTD calculation includes whole optical phenomena such as interference and diffraction effects. Details of the methods are given by Taflove and Hagness [15]. We used commercial FDTD software, FULLWAVE version 6.1 (Rsoft Inc.), for light reflection simulation.

Light was incident from the top of the cell and propagated for the z direction. We assume a periodic boundary condition for x direction and a perfect matching layer for z direction. Mesh size in the FDTD calculation is 5 nm for all directions. Both polarizations of incident light (TE and TM) were considered, and the reflection spectra of the samples for each polarization were averaged after each calculation.

Another numerical calculation method was also used in this work. We used a two-dimensional ray tracing method because of the shorter calculation time than the FDTD calculation. The method relies on geometric optics; thus, in contrast to the FDTD method, no wave optics effects such as interference are introduced in the ray tracing calculation. Details of the ray tracing methods are described in literature [16].

The ray tracing program was written in our laboratory using MATLAB R2009a (The MathWorks Inc.). We hypothesized that the sample boundary in the plane direction was the periodic boundary condition. Incident light to the sample was divided into 100 rays and irradiated on the unit area. Total reflected light from the sample surface was summarized to evaluate the reflectance.

4. Results and Discussions

4.1. Surface Morphology of the TiO_2 Sol-Gel Films. We initially investigated surface morphology and optical properties of the spin-coated TiO_2 films deposited on the alkaline textured silicon wafers. Figure 1 shows a cross-sectional SEM image of the spin-coated TiO_2 films using an as-received TiO_2 solution. The figure indicates that cracks occur near the grooves of the textured area. This is because the gel shrinks and cracks mainly at the groove of the pyramid, when the spin-coated TiO_2 gel is heat-burned in the furnace. Other researchers [12] have also pointed out the same phenomenon.

To reduce the cracking of the TiO_2 films, we changed the TiO_2 concentration of the sol-gel solution by diluting the solution with ethanol. Figures 2(a)–2(f) show SEM images of the top and cross-sectional views of the textured wafers with TiO_2 films prepared by using different starting solutions. Figure 2(c) shows that there are many cracks at the groove of the textured structures, where we used the solution that involves 3% TiO_2. On the other hand, when we used the solution with 1% TiO_2, there were few cracks, as indicated in Figure 2(a). This is because the TiO_2 film becomes thinner in this condition.

Figure 3 indicates experimental results of the light reflectance spectra of the textured substrates with TiO_2 sol-gel deposited films that are made from different solutions. The figure indicates that light reflectance barely depends on TiO_2 concentration of precursor solutions between 3% and 1%. On the other hand, the films using a 0.5% TiO_2 solution show higher reflectance, because the deposited films are too thin to work as an effective ARC.

On the basis of the above results, in the following experiments we used the sol-gel solution, which involves 1% of TiO_2. Next, we investigated the surface distribution of the spin-coated TiO_2 films on the textured area. Figures 4(a) and 4(b) show the cross-sectional SEM images and energy dispersive X-ray spectrometry (EDS) images of the textured surface with sol-gel deposited TiO_2 layers. The distributed area of Ti atoms in the EDS images corresponds to the covered area of the TiO_2 film. Figures 4(c) and 4(d) show top views of SEM and EDS images. The images indicate that there are fewer Ti atoms on the apex of the pyramid and that TiO_2 films are mainly deposited at the groove.

4.2. Optical Properties of the TiO_2 Sol-Gel Films. To highlight the optically noninterference behaviors of sol-gel deposited films, we measured light reflection spectra of the textured substrates with ARC films deposited by two different coating methods: RF magnetron sputtering and sol-gel spin-coating. In Figure 5(a), TiO_2 films were deposited onto the textured substrates using an RF magnetron sputtering method. We can clearly see the minimum value of reflectance due to interference at wavelengths around 600 nm. On the other hand, for the TiO_2 films prepared by the sol-gel method, Figure 5(b) indicates that light reflection is reduced in the entire visible region without interference. The thickness fluctuation of the deposited TiO_2 films, which is shown in Figure 5(b), cancels out the interference of light, and light reflection reduces uniformly.

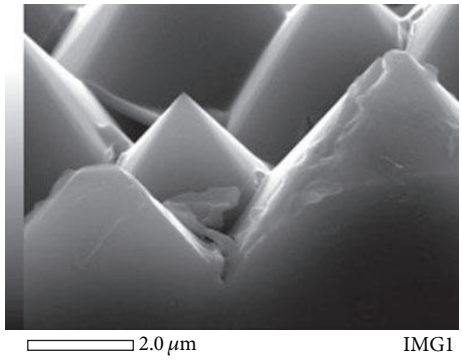

Figure 1: Cross-sectional SEM image of the spin-coated TiO_2 films on the textured surface. (TiO_2 concentration is 3%.)

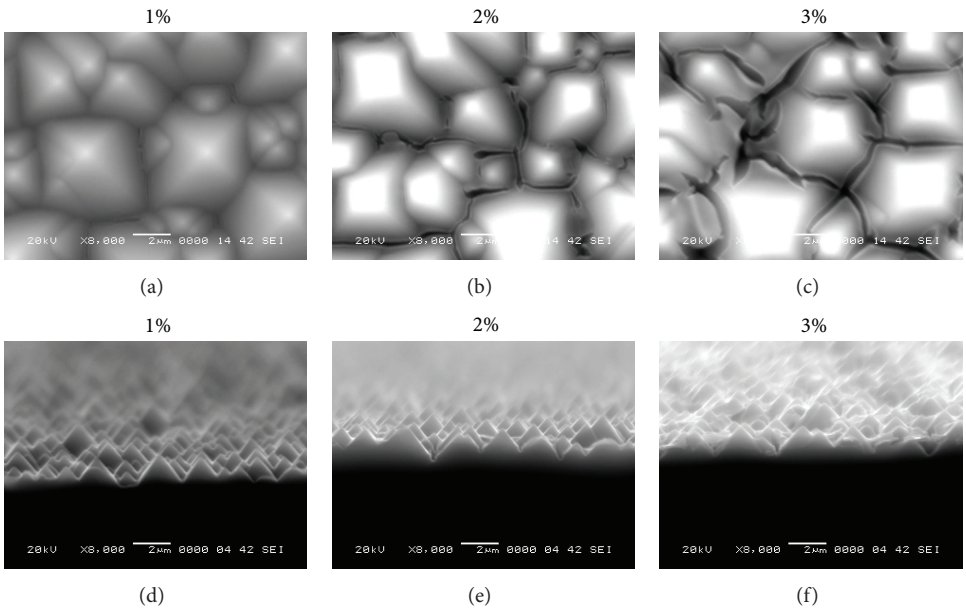

Figure 2: SEM images of the spin-coated TiO_2 films for different starting solutions. (a)–(c) Top view. (d)–(f) Cross-sectional view.

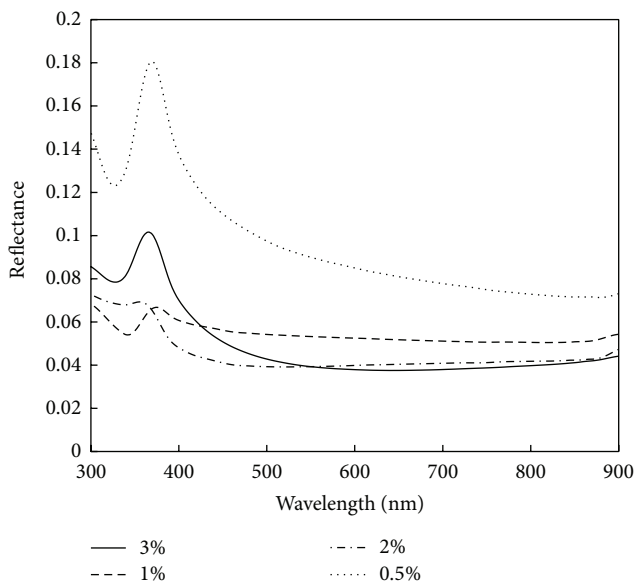

Figure 3: Dependence of reflectance spectra for different sol-gel solutions, which include various concentrations of TiO_2.

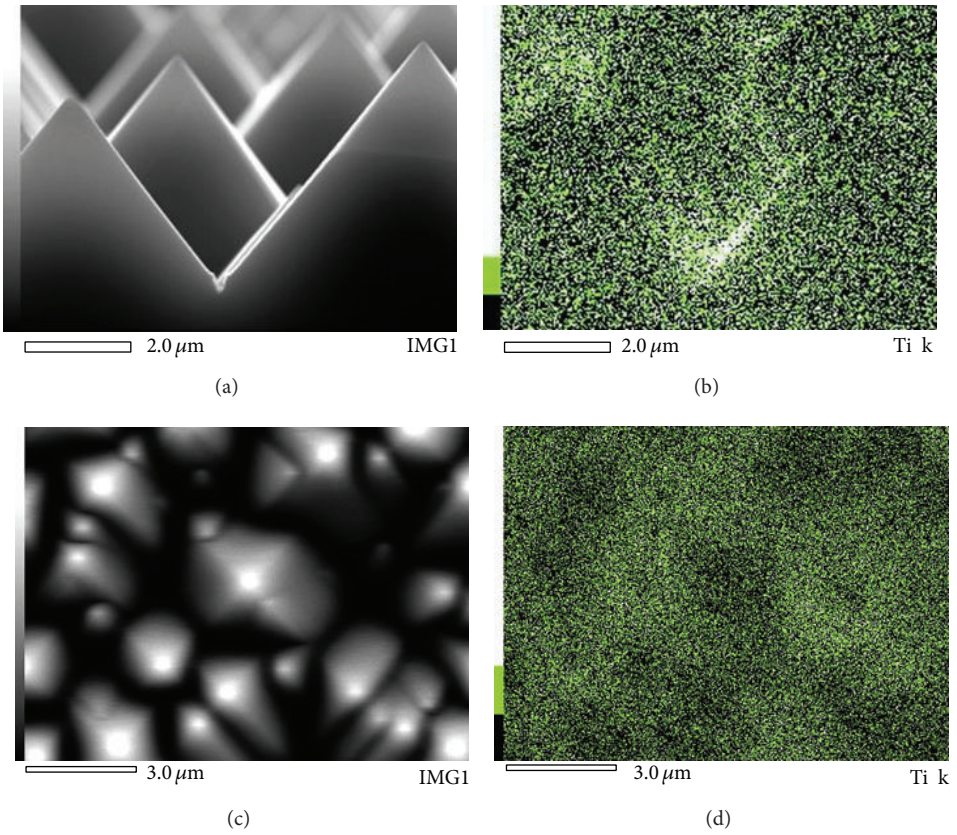

FIGURE 4: SEM and EDS images of the spin-coated TiO_2 films for 1% solution. (a)-(b) Cross-sectional view. (c)-(d) Top view.

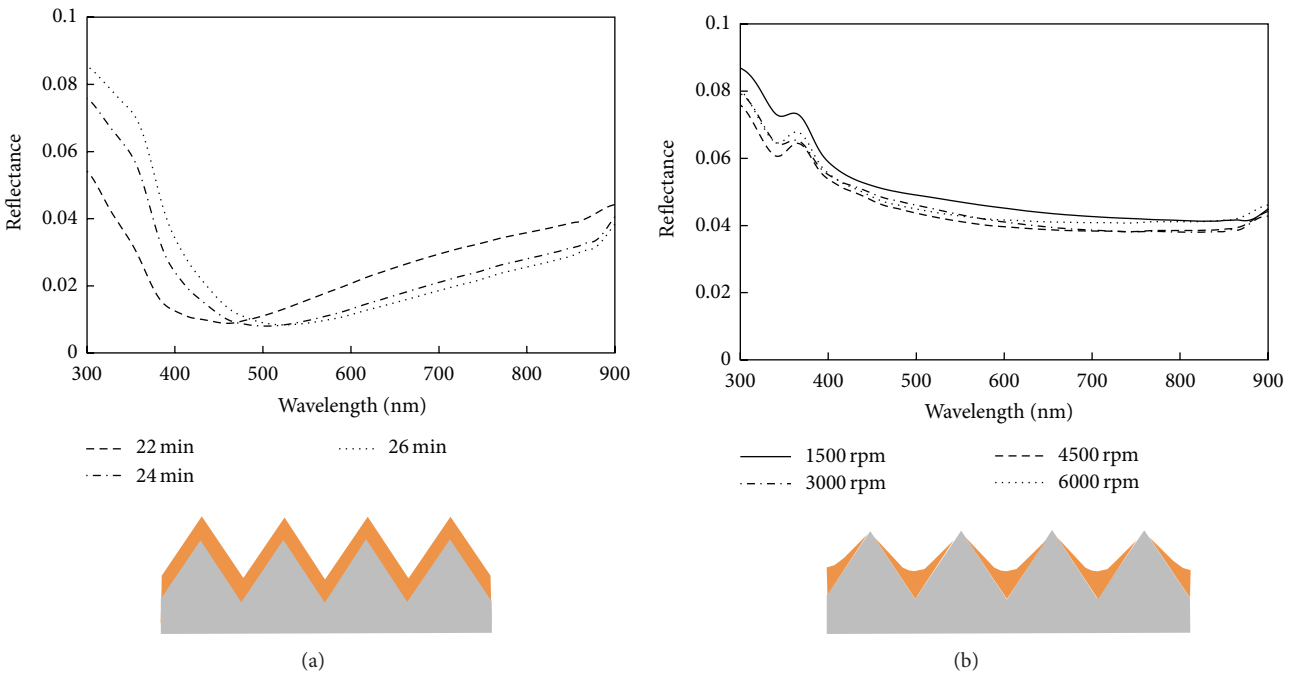

FIGURE 5: Measured reflection spectra from the textured surface with different TiO_2 ARC structures. (a) ARC films prepared by RF magnetron sputtering. Interference occurs for the wavelength of around 500 nm. (b) The films prepared by spin-coated method. There is no interference.

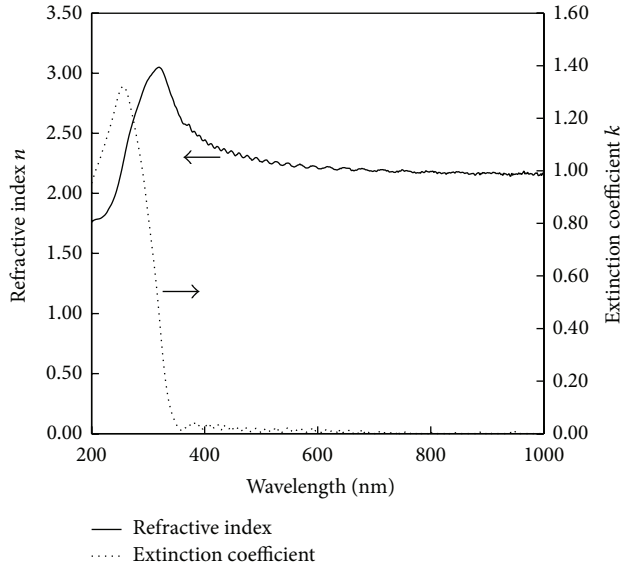

Figure 6: Measured refractive indices of TiO_2 films prepared by spin-coated method.

To evaluate the interference effect of the nonuniformly deposited sol-gel films, we numerically calculated reflection spectra using a two-dimensional FDTD method. We consider two different profiles of TiO_2 films on flat crystalline Si surfaces shown in Figure 7. Refractive indices of silicon are referenced from [17], and those of TiO_2 were measured with a spectroscopic ellipsometer. Obtained index values of TiO_2 are shown in Figure 6. Figure 7(a) shows calculated reflectance spectra of the flat TiO_2 layer on the Si substrates. We can clearly see that the reflection minimizes at the wavelengths around 600 nm due to the interference effect. On the other hand, in Figure 7(b), when the TiO_2 film is obliquely deposited on the substrate, reflectance of the sample decreases in the entire visible range. The calculation results also indicate that the interference effect is canceled out when thickness fluctuates slightly (200 to 300 nm) within TiO_2 film.

When TiO_2 film is deposited onto the textured substrates by a spin-coating method, there are thickness fluctuations in the deposited layer. Therefore, to evaluate the light reflection spectra of the textured wafers with a spin-coated TiO_2 layer, we can ignore the interference effect and use a ray tracing method instead of the time-consuming FDTD method.

4.3. Comparison of Experiment and Calculation. We performed a ray tracing calculation and compared experimental results with calculated results to understand the optical properties of the sol-gel deposited films on the textured substrates. At first, we modeled the structures of the sol-gel deposited nonuniform films for ray tracing calculation. Figure 8(a) shows an enlarged cross-sectional SEM image near the groove of the pyramidal structure. A puddle of TiO_2 is found at the groove in Figure 8(a). From the SEM image, we evaluated the puddle to be 320 nm thick and the pyramidal structures to be 2 μm high. Using these values, we modeled the cross-sectional structure of the sol-gel deposited film on the textured structure shown in Figure 8(b). In the model, surface morphology of the puddle was assumed to be a quadratic function. Since Figure 4 indicates that TiO_2 films do not fully cover the textured surfaces, we also consider the surface coverage, Y/X, in the ray tracing calculation. It is important to consider the ratio of the structure instead of its actual length because both calculation and experimental results satisfy the scaling law in noninterference conditions. Therefore, we focused on the ratio, Y/X, in the calculation.

Figure 9 shows the calculated reflectance of the textured surface with the nonuniform TiO_2 film. The values indicated in the figure are the ratio, Z/X, defined in Figure 8(b). In this calculation, surface coverage of the TiO_2 layers, Y/X, in the area is assumed to be 50%. Both experimental and numerically calculated reflectance spectra are shown in Figure 9. When the ratio, Z/X, is approximately equal to 0.1, calculated values roughly agree with experimental values.

Figure 10(a) indicates the plot of reflectance versus the ratio, Z/X. Light reflectance decreases as the ratio Z/X decreases. Figure 10(b) shows the reflectance versus surface coverage, Y/X. As surface coverage of the film increases, reflectance decreases from the surfaces. These results indicate that we need to prepare the films, which fully cover the textured area uniformly, to enhance the right reflection reduction further. However, to prepare fully covered and uniform films by the sol-gel method is the subject of further study.

5. Conclusion

We investigated morphology and optical properties of the spin-coated TiO_2 thin films on alkaline textured single-crystalline Si substrates. Thickness of spin-coated layer is

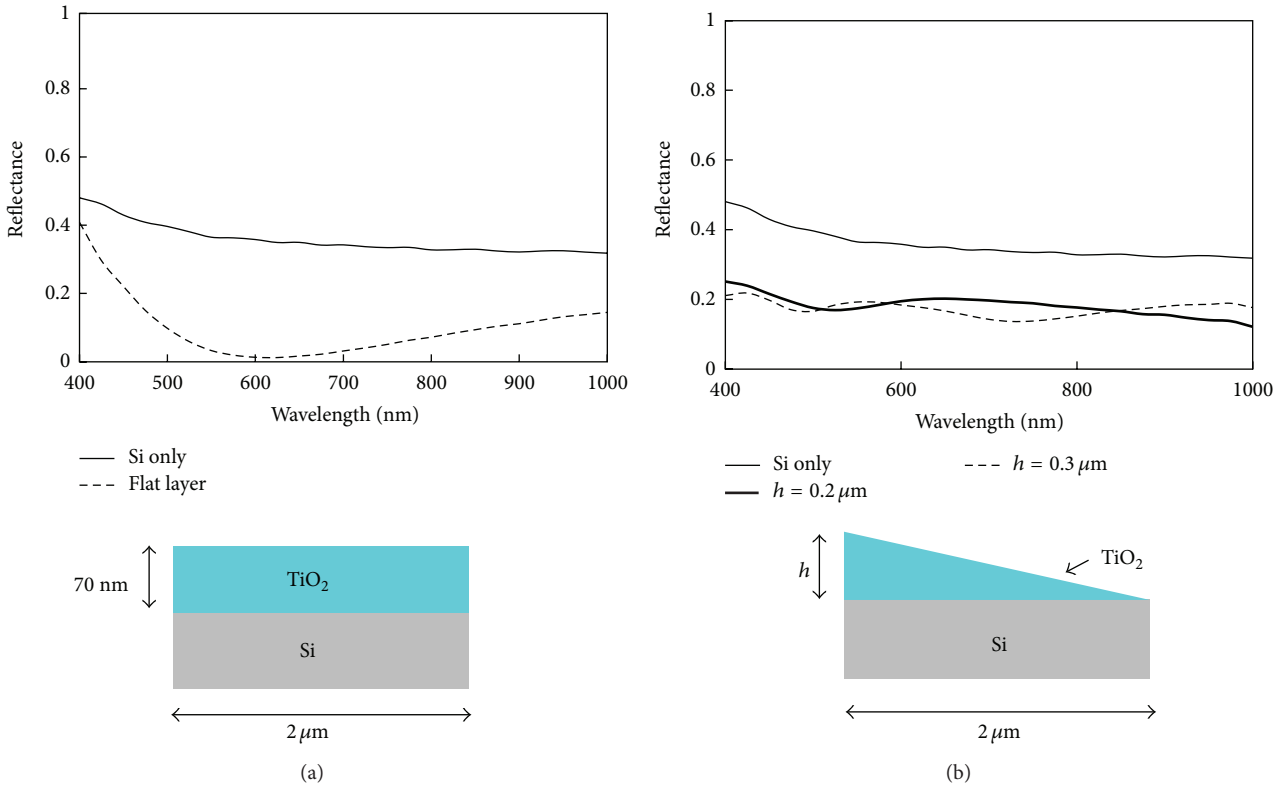

FIGURE 7: Calculated reflectance spectra from flat Si surfaces with different shapes of TiO_2 ARC structures. (a) Flat TiO_2 AR film. (b) Obliquely deposited film.

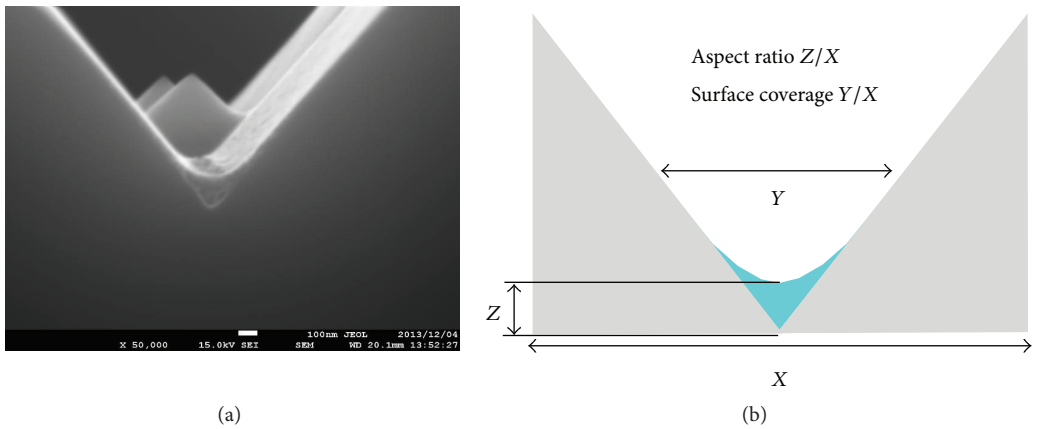

FIGURE 8: Expanded cross-sectional images of the pyramidal textured structures with puddle of TiO_2. (a) SEM image. (b) Model for ray tracing calculation.

nonuniform, and puddles of TiO_2 are formed at the groove of the textured structure. There was no interference in visible reflectance spectra and light reflection reduced uniformly in the experiment. We calculated the reflectance of the sol-gel deposited films on the textured surface using a ray tracing method. The calculated results agree well with experimental results in our conditions. This is because nonuniformly deposited films cancel out interference of light to uniformly reduce the reflection in the visible range. The calculation results indicate that puddle thickness must be reduced and the coverage area of the films increased to further reduce the light reflection of the surface of the textured wafers.

A spin-coated ARC layer on an alkaline textured Si surface is effective. To reduce the light reflectance of the spin-coated ARC films further, we need to improve the uniformity of the films.

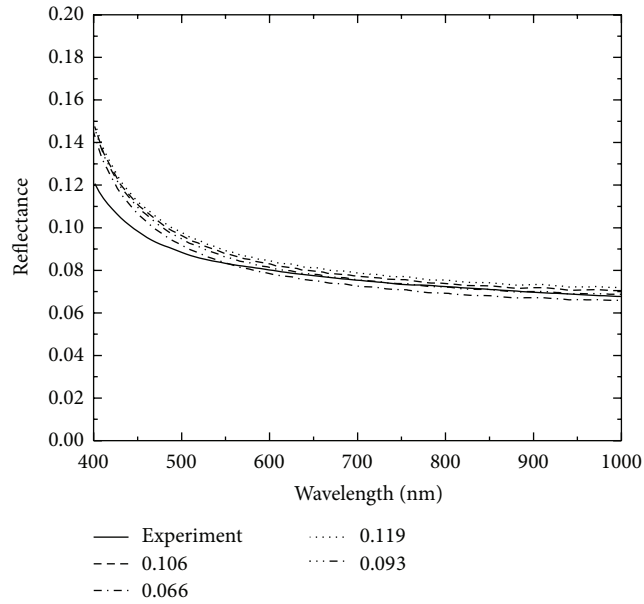

Figure 9: Dependence of experimental and calculated reflectance spectra from the textured Si surface with spin-coated TiO_2 layer on aspect ratio, Z/X. In numerical calculation, surface coverage of TiO_2 is assumed to be 50%.

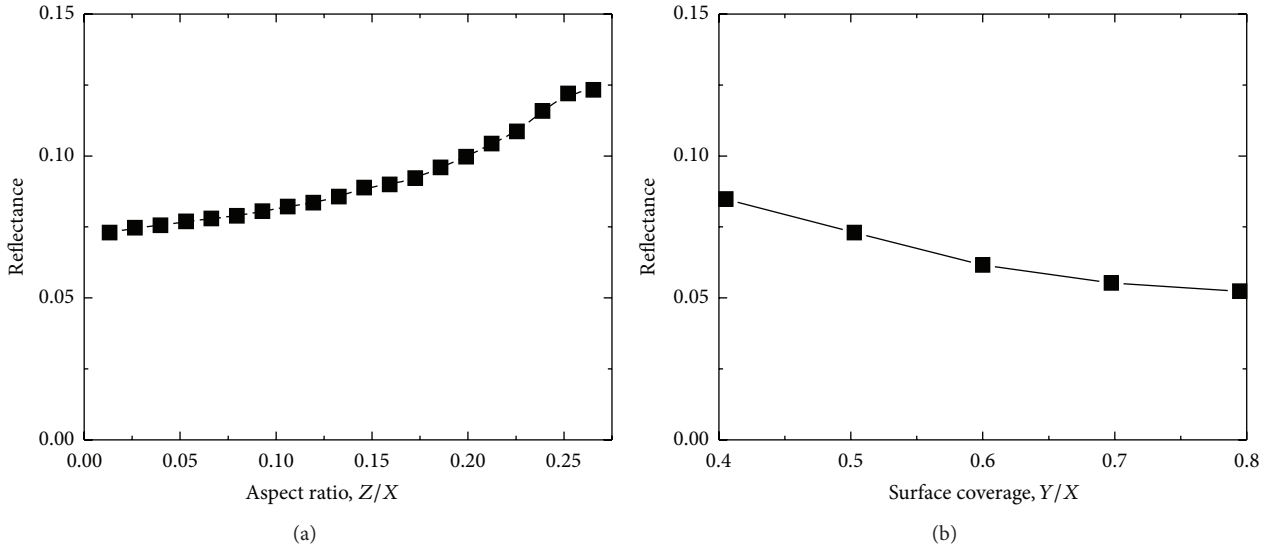

Figure 10: Calculated reflectance ($\lambda = 600$ nm) as a function of (a) puddle thickness, Z/X, and (b) surface coverage, Y/X.

Conflict of Interests

The authors declare that there is no conflict of interests regarding the publication of this paper.

Acknowledgments

The authors gratefully thank Dr. Akio Higo of Tohoku University for his help with FDTD numerical calculations. They are grateful to Professor Takashi Sakai of Seikei University for his help with SEM and EDS measurements. They also thank Yasuhito Nakai and Kazuhisa Umemoto for their support in the experiment. Ellipsometry measurement was carried out in the Research Hub for Advanced Nano Characterization, the University of Tokyo, supported by the Ministry of Education, Culture, Sports, Science and Technology (MEXT), Japan.

References

[1] L. Martinu and D. Poitras, "Plasma deposition of optical films and coatings: a review," *Journal of Vacuum Science and Technology A: Vacuum, Surfaces and Films*, vol. 18, no. 6, pp. 2619–2645, 2000.

[2] C. Martinet, V. Paillard, A. Gagnaire, and J. Joseph, "Deposition of SiO_2 and TiO_2 thin films by plasma enhanced chemical vapor deposition for antireflection coating," *Journal of Non-Crystalline Solids*, vol. 216, pp. 77–82, 1997.

[3] P. Doshi, G. E. Jellison Jr., and A. Rohatgi, "Characterization and optimization of absorbing plasma-enhanced chemical vapor deposited antireflection coatings for silicon photovoltaics," *Applied Optics*, vol. 36, no. 30, pp. 7826–7837, 1997.

[4] S. Duttagupta, F. Ma, B. Hoex, T. Mueller, and A. G. Aberle, "Optimised antireflection coatings using silicon nitride on textured silicon surfaces based on measurements and multidimensional modelling," *Energy Procedia*, vol. 15, pp. 78–83, 2012.

[5] B. Vallejo, M. Gonzalez-Mañas, J. Martínez-López, F. Morales, and M. A. Caballero, "Characterization of TiO2 deposited on textured silicon wafers by atmospheric pressure chemical vapour deposition," *Solar Energy Materials and Solar Cells*, vol. 86, no. 3, pp. 299–308, 2005.

[6] D. Chen, "Anti-reflection (AR) coatings made by sol-gel processes: a review," *Solar Energy Materials & Solar Cells*, vol. 68, no. 3-4, pp. 313–336, 2001.

[7] P. Nostell, A. Roos, and B. Karlsson, "Optical and mechanical properties of sol-gel antireflective films for solar energy applications," *Thin Solid Films*, vol. 351, no. 1-2, pp. 170–175, 1999.

[8] G. San Vicente, A. Morales, and M. T. Gutierrez, "Preparation and characterization of sol-gel TiO_2 antireflective coatings for silicon," *Thin Solid Films*, vol. 391, no. 1, pp. 133–137, 2001.

[9] N. Batra, P. Kumar, S. K. Srivastava et al., "Controlled synthesis and characteristics of antireflection coatings of TiO_2 produced from a organometallic colloid," *Materials Chemistry and Physics*, vol. 130, no. 3, pp. 1061–1065, 2011.

[10] G. San Vicente, A. Morales, and M. T. Gutiérrez, "Sol-gel TiO_2 antireflective films for textured monocrystalline silicon solar cells," *Thin Solid Films*, vol. 403-404, pp. 335–338, 2002.

[11] N. H. Arabi, A. Iratni, H. El Hamzaoui et al., "Antireflective sol-gel TiO_2 thin films for single crystal silicon and textured polycrystal silicon," *Journal of Sol-Gel Science and Technology*, vol. 62, no. 1, pp. 24–30, 2012.

[12] A. M. Petersson, P. Lindberg, and T. Boström, "Optical and passivating properties of sol-gel derived silica and titania coatings on textured monocrystalline silicon," in *Proceedings of the 37th IEEE Photovoltaic Specialists Conference (PVSC '11)*, pp. 002918–002923, Seattle, Wash, USA, June 2011.

[13] C. H. Yang, S. Y. Lien, C. H. Chu, C. Y. Kung, T. F. Cheng, and P. T. Chen, "Effectively improved SiO_2-TiO_2 composite films applied in commercial multicrystalline silicon solar cells," *International Journal of Photoenergy*, vol. 2013, Article ID 823254, 8 pages, 2013.

[14] D. L. King and M. E. Buck, "Experimental optimization of an anisotropic etching process for random texturization of silicon solar cells," in *Proceedings of the 22nd IEEE Photovoltaic Specialists Conference (PVSC '91)*, pp. 303–308, October 1991.

[15] A. Taflove and S. C. Hagness, *Computational Electrodynamics: The Finite-Difference Time-Domain Method*, Artech House, Boston, Mass, USA, 3rd edition, 2000.

[16] S. A. Glassner, Ed., *An Introduction to Ray Tracing*, Morgan Kaufmann, San Francisco, Calif, USA, 1989.

[17] D. E. Palik, *Handbook of Optical Constants of Solids*, Elsevier, 1998.